

NEW HYBRID SILVER COLLOID-A₃B PORPHYRIN COMPLEX EXHIBITING WIDE BAND ABSORPTION

I. CREANGA^a, G. FAGADAR-COSMA^{b*}, A. PALADE^a, A. LASCU^a,
C. ENACHE^a, M. BIRDEANU^c, E. FAGADAR-COSMA^a

^a*Institute of Chemistry Timisoara of Romanian Academy, 24 M. Viteazu Ave, 300223-Timisoara, Romania*

^b*"Politehnica" University of Timisoara, Faculty of Industrial Chemistry and Environmental Engineering, Victoriei Square 2, 300006-Timisoara, Romania,*

^c*National Institute for Research and Development in Electrochemistry and Condensed Matter, 1 Plautius Andronescu Street, 300224-Timisoara, Romania*

The reduction of silver ions by citrate, using different molar ratios, was done to synthesize colloidal systems consisting in spherical and ovoid disk-shaped silver nanoparticles in solution, with sizes in the range of 30-49 and 65-120 nm, respectively. The reaction is characterized by measuring the silver ion concentration and by UV-vis, fluorescence and atomic force microscopy (AFM). Active junction between the Ag colloids and the A₃B porphyrin, namely: 5,10,15-tris-(4-pyridyl)-20-(3,4-dimethoxy-phenyl)-porphyrin (TPyDMPP) was investigated in acidic medium. The effect of functional groups grafted on porphyrin on the linkage type in the hybrid system is envisaged. The electrostatic interactions between protonated positively charged porphyrins to the negatively charged Ag colloid explain the complex generation. The optical properties of hybrid Ag colloid-porphyrin system can be tuned over a wide spectral range as a function of nanoparticles size, shape, mutual interactions and spatial ordering of particles, to exploit the versatile properties of these systems in sensors design and as photosensitizers in PDT and in photovoltaic cells. Another target was to use these materials for investigation of antibacterial performance.

(Received February 25, 2013; Accepted March 23, 2013)

Keywords: hybrid nanomaterial, silver colloid, A₃B mixed substituted porphyrin, UV-vis absorption, AFM

1. Introduction

Obtaining and characterization of hybrid multifunctional materials based on porphyrins containing silver nanoparticles, usually stabilized by polymer networks, have recently received well deserved interest in the design of sensors, biocidal products, bio-materials, and other drug supports [1-3]

Regarding porphyrin-silver colloid hybrid fluorescent systems, the most important aspect that influences the type of linkage to the silver colloid is the core structure and the nature of the side substituents that are attached to the porphyrin ring.

Silver nanosized particles received increased interest due to their high surface-to-volume ratio and their versatile shape/size dependent properties and can be obtained either by physical or by chemical means. The selection of the method highly depends on the desired particle size and on the further use of the obtained material. [4].

*Corresponding author: gfagadar@yahoo.com

The physical methods imply high energy consumption and therefore many researchers prefer the chemical production of nanoparticles that also allows the tight control over size. In principle, a silver salt is reduced to neutral silver and this is to be surrounded by stabilizing agents, in order to maintain a low aggregation. The most commonly used silver salt is silver nitrate and the reducing agents vary from softer sodium citrate [5] to the more drastic sodium borohydride [6]. Each procedure is targeted on the further application of the colloid such as: sensor formulations [7], optical data storage, diverse catalytic activities, medical regenerative actions (improvement patterns of re-epithelialisation, wound closure and healing), antifungal and anti-bacterial activity (agents in textile coatings, medical and water treatments, food storage, and construction of air purification devices) [8-10].

Silver nanoparticles can be synthesized as pure silver or in various hybrids. New trends include the incorporation of silver ions into new amorphous hybrid materials prepared by the sol-gel method, based on SiO_2 and hydroxypropyl cellulose and used for the investigation of antibacterial performance against *E. coli* and *B. subtilis* [11]. Ag nanoparticles impregnated by sol-gel in mercaptopropyltrimethoxysilane were used for a highly sensitive voltammetric sensor for monitoring free cyanide [12]. Silver-doped glass and ceramics are expected to be candidates for antibacterial materials against Gram-positive *Staphylococcus aureus* and Gram-negative *Escherichia coli* bacteria [13].

In order to control the aggregation of the particles, sometimes a double reduction is preferred, both sodium citrate and sodium borohydride being used [14]. In most recent literature the interest is focused on obtaining nanoparticles with the help of more available and non-polluting natural materials, so a large variety of natural extracts were used to obtain the necessary stability of the nanosized metal: the reduction with banana peel extract [15] aqueous extract of *Solanum torvum* fruit [16] in which case spherical shapes with smooth surface are obtained; the combination of ascorbic acid and starch was also tested with excellent results [17].

Colloidal solutions tend to coagulate so their stability is a considerable issue. Poly(vinyl alcohol), poly(vinylpyrrolidone) and sodium dodecyl sulfate have been used to solve this coagulation problem and to obtain nano silver with narrow size distribution embedded in a polymeric matrix [18].

The shape of the colloidal silver can also be tuned from spherical with diameters ranging from 10 to 50 nm [19] to nanodisks type [14].

Silver colloids stabilized by cellulose, glass, and quartz supports can be stable for more than 3 weeks [20].

In our case the interest was to use the silver colloidal nanoparticles for the coordination with porphyrin derivatives, so that bulky stabilizing agents are not very welcomed. For obtaining the silver colloid we chose the reduction with sodium citrate at boiling [21, 22] analyzing the influence of various concentrations of the citrate solution both on the distribution of particle sizes and on the intensity absorption of the plasmon.

In connection to our previously reported wide-band absorption advanced hybrid materials based on porphyrin [22, 23-25] the major purpose of the present work was to obtain new multifunctional hybrids, to analyze and interpret the possible changes produced by conjugation of a new mixed substituted A_3B porphyrin, namely 5,10,15-tris-(4-pyridyl)-20-(3,4-dimethoxyphenyl)-porphyrin on the surface of Ag colloidal particles.

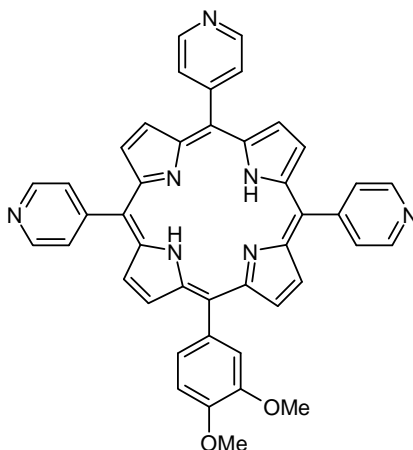


Fig. 1. Structure of 5,10,15-tris-(4-pyridyl)-20-(3,4-dimethoxy-phenyl)-porphyrin

The conjugation of a porphyrin to the surface of a metal colloid can be realized by several means: binding of the porphyrin core to the surface of the Ag particle through ligand binding; electrostatic interactions between protonated positively charged porphyrins to the negatively charged Ag colloid; covalent binding by functional groups of porphyrins; non-covalent, affinity-based host-guest systems.

Most biomolecules used to be conjugated on the surface of a metal colloid possess a carboxylic acid group or an amine group [26]

2. Experimental

Materials. The reagents were of the highest purity obtainable from Merck and Scharlau (Germany) and were used without further purification. The novel mixed substituted porphyrin, namely: 5,10,15-tris-(4-pyridyl)-20-(3,4-dimethoxy-phenyl)-porphyrin was obtained by multicomponent synthesis, modifying previously reported method [27]

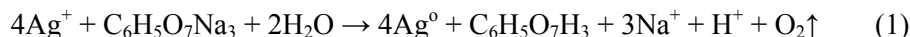
General methods for obtaining of silver colloids: Silver nitrate, 18 mg (0.105×10^{-3} mol) was solved in 100 mL distilled water. The solution is heated to boiling and various amounts of sodium citrate solution (0.5% wt), in molar ratios silver nitrate/ sodium citrate = 1:1.62 ÷ 1:0.32 are added dropwise under intense stirring (1200 rot/min). The boiling and stirring are maintained for 1 h and then the solution is cooled to room temperature and UV-vis spectrum is recorded. Sample 1 was obtained by using 10 mL (0.17×10^{-3} mol) sodium citrate solution and Sample 2 by adding 2 mL (0.034×10^{-3} mol) sodium citrate solution (0.5% wt).

Apparatus. Nanosurf[®] EasyScan 2 Advanced Research AFM (Switzerland), equipped with a stiff ($450 \mu\text{m} \times 50 \mu\text{m} \times 2 \mu\text{m}$) piezoelectric ceramic cantilever (spring constant of $0.2 \text{ N}\cdot\text{m}^{-1}$) with an integral tip oscillated near its resonance frequency of about 13 kHz was used for atomic force microscopy (AFM) measurements. The surface imaging investigations were done in ambient conditions with samples deposited onto pure silica plates by slow evaporation of the water-THF as solvent mixture. AFM images were obtained in contact mode and are quantitative on all three dimensions.

Fluorescence spectra were recorded in water-THF on a Perkin Elmer Model LS 55 apparatus (USA). The fluorescence spectra were recorded using slit widths of 11 nm for excitation, and 5 nm for emission, with a 290 nm cut-off filter. UV-visible spectra were recorded on a JASCO UV-visible spectrometer, V-650 model (Japan). Absorption, excitations and emission spectra were registered in environmental conditions (temperature: 20 ± 2 °C), on 1 cm path length cells.

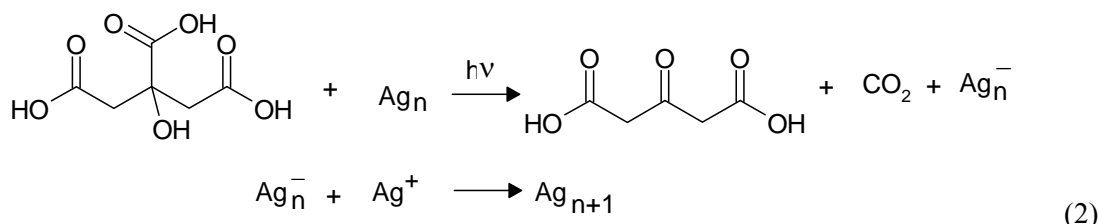
3. Results and discussions

The equation of the reaction (1) could be expressed as follows [21]:



Citrate molecules play a double role, both as a capping ligand for the silver particles and as a photoreducing agent for the silver ions. Two carboxylic groups from citrate are binding to the silver surface and the last one is normal to the surface, being responsible for the colloid stabilization by electrostatic repulsion [28].

Besides, the carboxylic groups when absorbing on silver act as nucleophilic agents and generate a partial electron transfer producing a negative charge (equation 2), generating CO_2 and acetone-1,3 dicarboxylate.



Regarding the electronic spectra, it was observed that with the particles increasing in size, the absorption peak is bathochromically shifted [29]

The absorbance of spherical silver nanoparticles in water was calculated [30] by a summation of the Gustav Mie series and modifications [31] including multipoles ≤ 10 , for different particle sizes in the range from 3 to 80 nm (Table 1).

The calculated maximum absorption of silver nanoparticles in water (considering a maximum absorbance of 2) as a function of particle radius shows a rise to a maximum as the particle size increases.

The bandwidth of the surface plasmon band of silver at half-maximum absorption was also evaluated as a function of particle radius. The number of particles per dm^3 decreases 10^{17} to 10^{13} in water, as the particle radius increases from 1.5 to 40 nm, respectively.

Table 1. The calculated characteristics of silver nanoparticles in water (considering a maximum absorbance of 2) as a function of particle radius.

Particle radius (nm)	Peak position nm	Maximum absorbance at conc. $10^{-5}\text{g/cm}^3 \text{Ag}^0$	The bandwidth of the surface plasmon absorption band of silver nanoparticles at half-maximum absorbance in water	Maximum number of silver nanoparticles in water $\text{dm}^3 \times 10^{15}$
5	400	0.8	70	35
10	405	1	55	0.8
15	410	1.1	55	0.12
20	415	1.2	55	0.08
25	425	1.1	60	0.06
30	435	1	65	0.04
35	445	0.8	75	0.02
40	455	0.6	95	0.01
45	465		110	

*** The data are according with calculations and diagrams from [30]

Increasing the silver content from 10^{-5}M to 10^{-4}M (Figure 2) it can be noticed that the intensity of the absorption peak becomes three times higher. Our results are in agreement with reported data [32] and we can state that the presumed reason for the bathochromic shift of Sample 2 is the formation of large size particles associated with a broadened size distribution, and even, as AFM studies revealed the ovoid shape of silver nanoparticles.

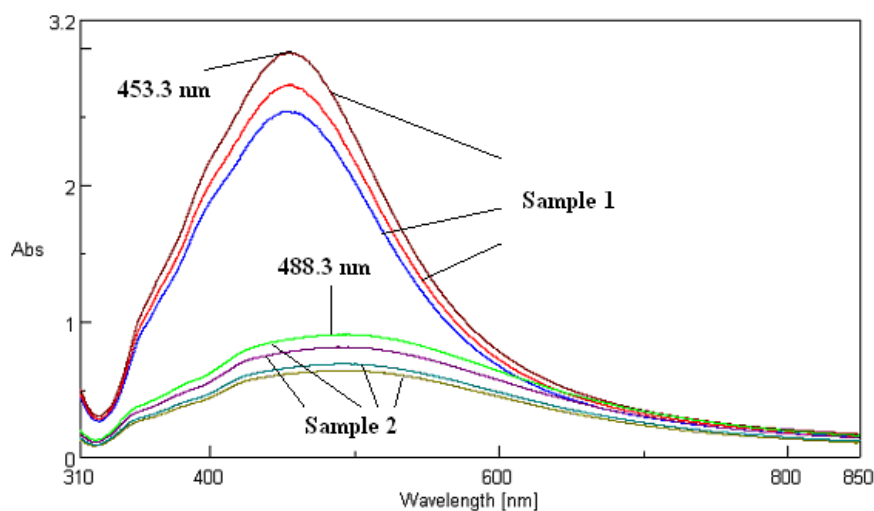


Fig. 2. Superposed UV-vis spectra for Ag colloid: Sample 1 ($c=10^{-4}$ M); Sample 2 ($c=10^{-5}$ M)

The UV-vis spectrum of 5,10,15-tris-(4-pyridyl)-20-(3,4-dimethoxy-phenyl)-porphyrin is characteristic to *etio* type class with the very intense Soret band at 423 nm accompanied in the visible region by four Q-bands decreasing in intensity (Figure 3). The Soret band is the result of transition from $a_{1u}(\pi) - e_g^*(\pi)$ and the four Q bands, located at 516, 553, 593 and 651 nm respectively are corresponding to $a_{2u}(\pi) - e_g^*(\pi)$ transitions.

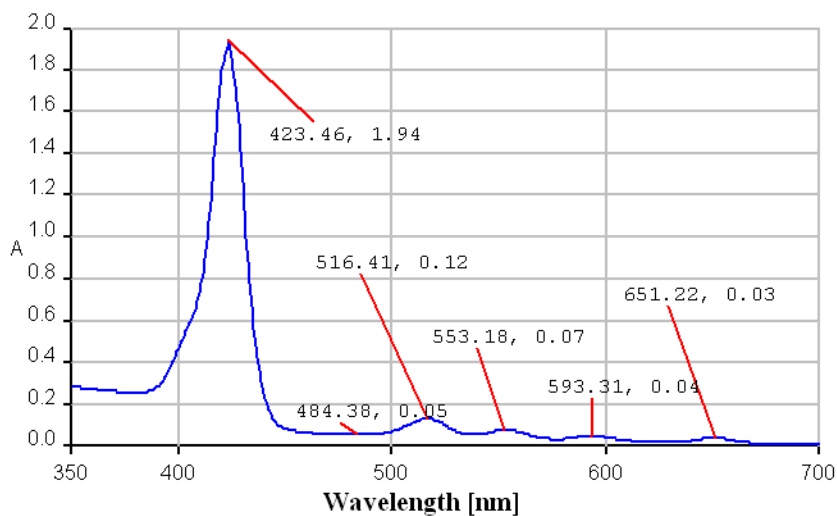


Fig. 3. UV-vis spectrum of the 5,10,15-tris-(4-pyridyl)-20-(3,4-dimethoxy-phenyl)-porphyrin

Active junction between the Ag colloids (Sample 1, 10^{-7} M) and 5,10,15-tris-(4-pyridyl)-20-(3,4-dimethoxy-phenyl)-porphyrin (Figure 4) was obtained by continuously adding small portions of 100 μ l porphyrin and 150 μ l HCl 0.1N, for protonating it in order to obtain rapid affinity between negatively charged silver colloid and protonated porphyrin.

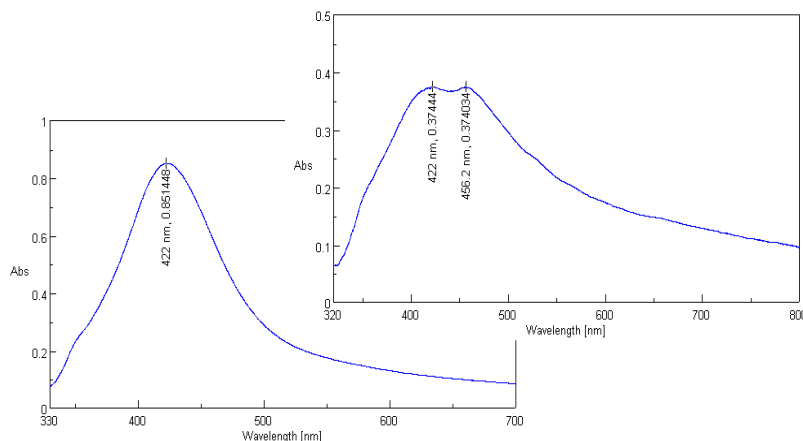


Fig. 4. UV-vis of initial Sample 1 colloid and first step of porphyrin-nanoAg complex formation

The formation of the complex has important features in UV-vis. By continuously adding of porphyrin to the silver colloid accompanied by an increase in acidity, the protonation of the inner nitrogen atoms of the porphyrin ring is produced (Figure 5).

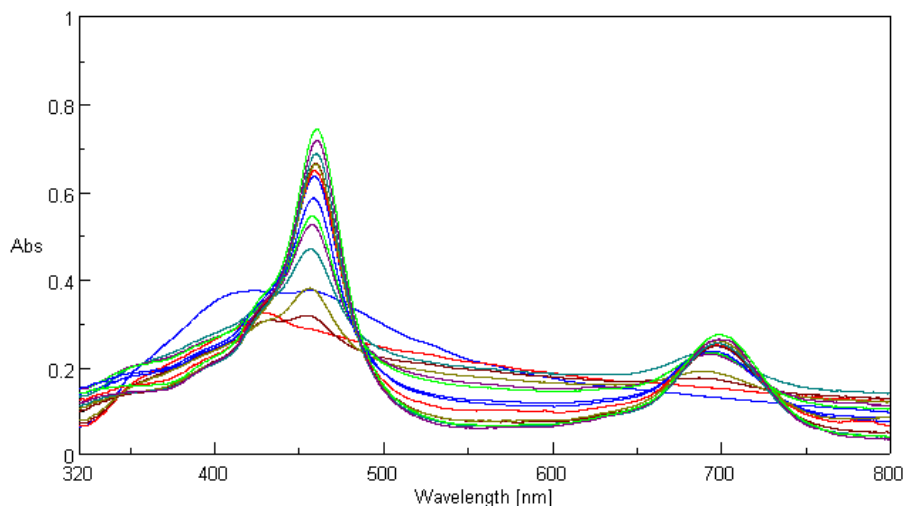
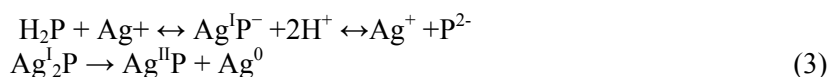


Fig. 5. Overlapped UV-vis of hybrid (TPyDMPP) porphyrin-nanoAg complex formation with wide-band absorption.

The spectra at measured pH between 4.5 to 2.5 from Figure 5 showed a Soret band that is broadened and red shifted from 423 nm (pH=5.5) to 460 nm accompanied by only one Q band, which is the QI band, also significantly bathochromic shifted to 700 nm. The QI band has also suffered important hyperchromic effects. By its whole, the complex presents wide absorption from 320 nm to 750 nm, thus making this material a remarkable photosensitizer.

We may supplementary notice that some J-aggregates have been formed, also explained by the UV-vis shape, especially the broadened red-shifted absorption band [27]. Based on the fact that the hybrid formation is accompanied by four isosbestic points, two on Soret and two on QI band, it seems likely that silver (I) ions may undergo disproportionation in the coordination cavity of the ligand, according with equation (3) and some recent reports [33].



This kind of disproportion reactions taking place inside the porphyrin core can produce a nonlinear calibration curve for the dependence on metal ion concentrations [34]. Besides, the pyridyl external groups can also be protonated and create favorable conditions for a dome distortion of positively charged porphyrin that can be attracted on the negative charge of the silver colloid surface.

So, in case of (TPyDMPP) porphyrin, the binding in the novel hybrid material can be easily explained by electrostatic interactions between protonated positively charged porphyrins to the negatively charged Ag colloid.

Emission spectra. The emission spectrum of bare 5,10,15-tris-(4-pyridyl)-20-(3,4-dimethoxy-phenyl)-porphyrin in water-HCl system, $c = 1 \times 10^{-5} \text{M}$ (Figure 6A) exhibits an intense and broad $Q_x(0,0)$ fluorescence band at 660nm and a weaker emission band situated at 725nm, assigned to $Q_x(0,1)$ transition.

The excitation spectrum of the bare porphyrin (Figure 6B), at λ_{em} of 660 nm at the same concentration, shows a splitting of the enlarged Soret band into two evident bands, with the first peak hypsochromically shifted and the second one bathochromically shifted, revealing a beginning of an aggregation process. The aggregation, according to this phenomenon is based both on H and J type mechanisms.

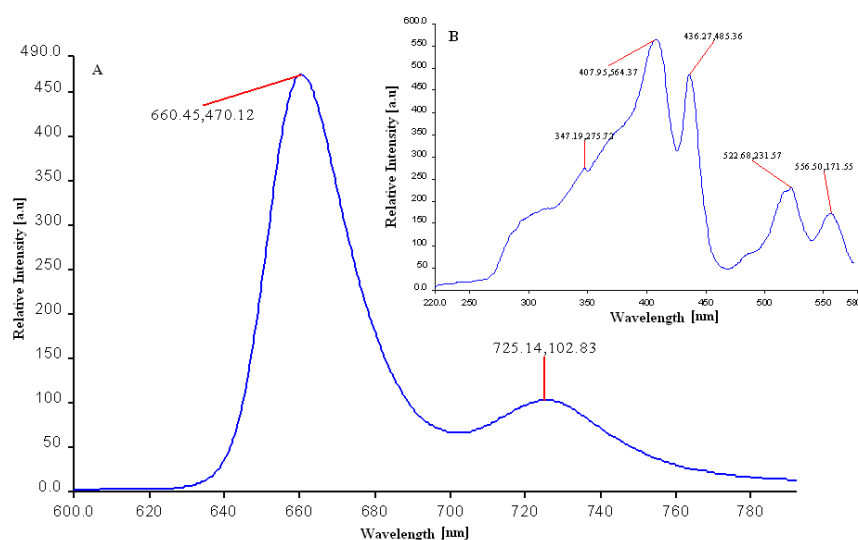


Fig. 6. Curve A: The emission spectrum of bare (TPyDMPP) porphyrin in water-HCl system, $\lambda_{ex} = 408 \text{ nm}$, and cut off filter 515 nm; Curve B: The excitation spectrum at λ_{em} of 660 nm, cut-off filter 515 nm.

The fluorescence emission spectrum of Ag colloid Sample 1 (Fig. 7) exhibits an intense band emitting in blue at 457 nm, which is accompanied by a small intensity band emitting in the red region, around 685 nm.

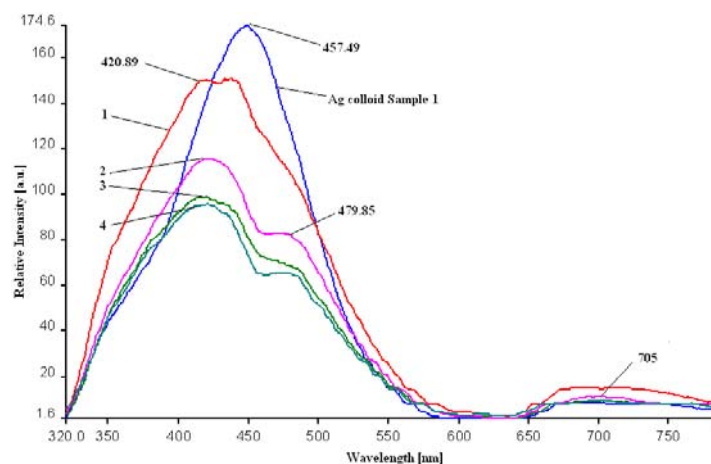


Fig. 7. Overlapped emission spectra of Ag colloid in comparison with spectra 1-4 of porphyrin-silver complex, in increasing order of porphyrin concentration, $\lambda_{ex} = 239$ nm, cut off filter 290nm

By continuously adding the (TPyDMPP) porphyrin (Figure 7 - curves 1-4), in acidic medium of HCl, this band is broadening and displaying a second peak, bathochromically shifted to 480 nm, assigned to porphyrin-silver complex, the peak assigned to non-complexed silver being shifted to blue, around 421 nm.

The generation of the hybrid silver-porphyrin nanomaterial can be also noticed in the emission spectra by the presence of the large band in the red region, around 705 nm, that is increasing in intensity, making from this nanomaterial a real candidate for PDT tests (second generation photosensitizer).

The AFM was performed for both Silver Colloid Sample 1 and also Sample 2 complexed with 5,10,15-tris-(4-pyridyl)-20-(3,4-dimethoxy-phenyl)-porphyrin (Figures 8-10). The major advantage of AFM is that it offers and quantitatively measures two and three – dimensional images, so that particle height and volume can be calculated and the topography of the surface can be analyzed.

In accordance with literature data [35] AFM analysis reveals the size reduction of the Ag nanoparticles due to the heat-treatment. The mechanism that may be presumed has two steps: by increasing the temperature, the silver particles on the surface diffuse into solution, being oxidized. The diffusion of the surface particles produces the average size decrease of the rest of the particles on the surface. In the case of Sample 1, we made complexation with porphyrin by heating and acid adding.

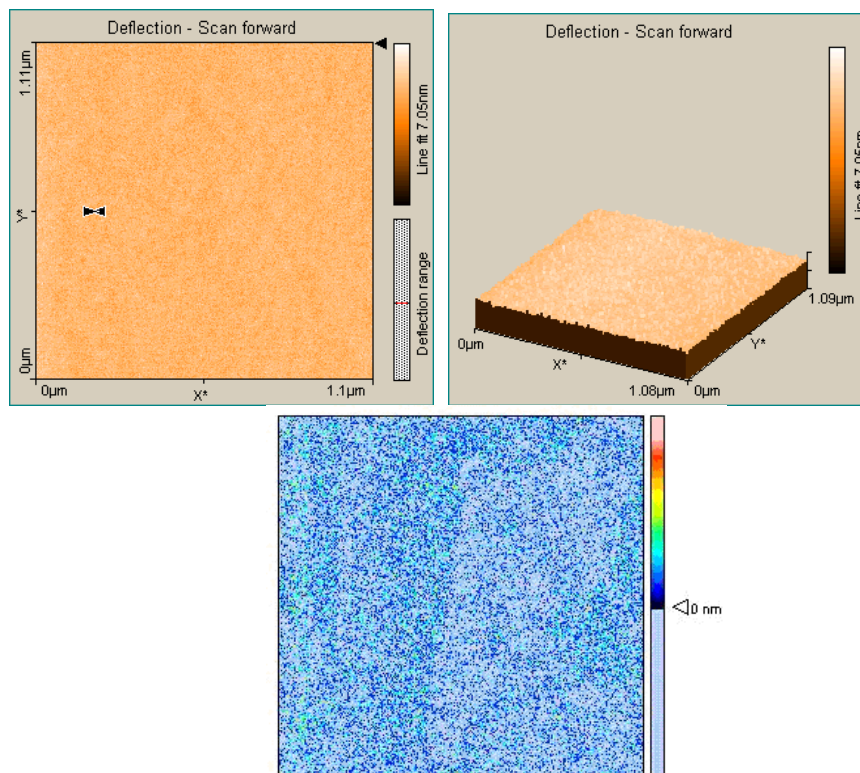


Fig. 8. 2D AFM image in contact mode and particle analysis of Sample 1 Ag colloid-complexed with (TPyDMPP) porphyrin.

The distribution of the particle size is in a narrow range of 30-49 nm (Sample 1). On pure silica surface of $1 \mu\text{m} \times 1 \mu\text{m}$ there are deposited a number of approx. 6000 particles with a mean height of islands of 0.4 nm and average volume of islands of 25.8 nm^3 .

AFM image of the dry surface of the hybrid (TPyDMPP) porphyrin -Ag colloid (Sample 2-Figure 9), reveals the formation of some pyramids, similar in shape with the hybrid structures formed by porphyrin -silica complexes.

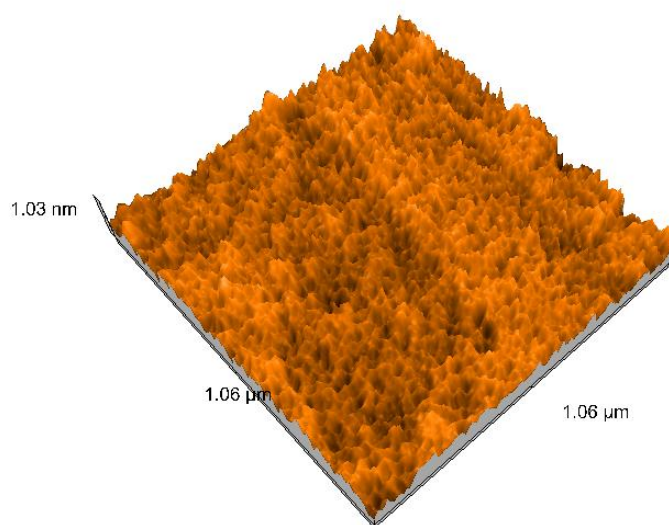


Fig. 9. 3D AFM image of the dry surface of the hybrid (TPyDMPP) porphyrin -Ag colloid (Sample 2)

Sample 2 composition consists in spherical and ovoid shaped Ag particles in the average range of 69-122 nm, but also ovoid silver particles exceeding 200 nm are present (Figure 10 a,b).

From the topographical point of view, surface roughness (S_a) is uniform, having a value of 97 nm and the maximum peak height (S_p) is also constant at 98nm (Figure 10 c).

Images of $1 \times 1 \mu\text{m}$ show cavities of 97 nm in diameter very uniform in shape and size. Maximum valley depth (S_v) is also in the same range, of 95 nm.

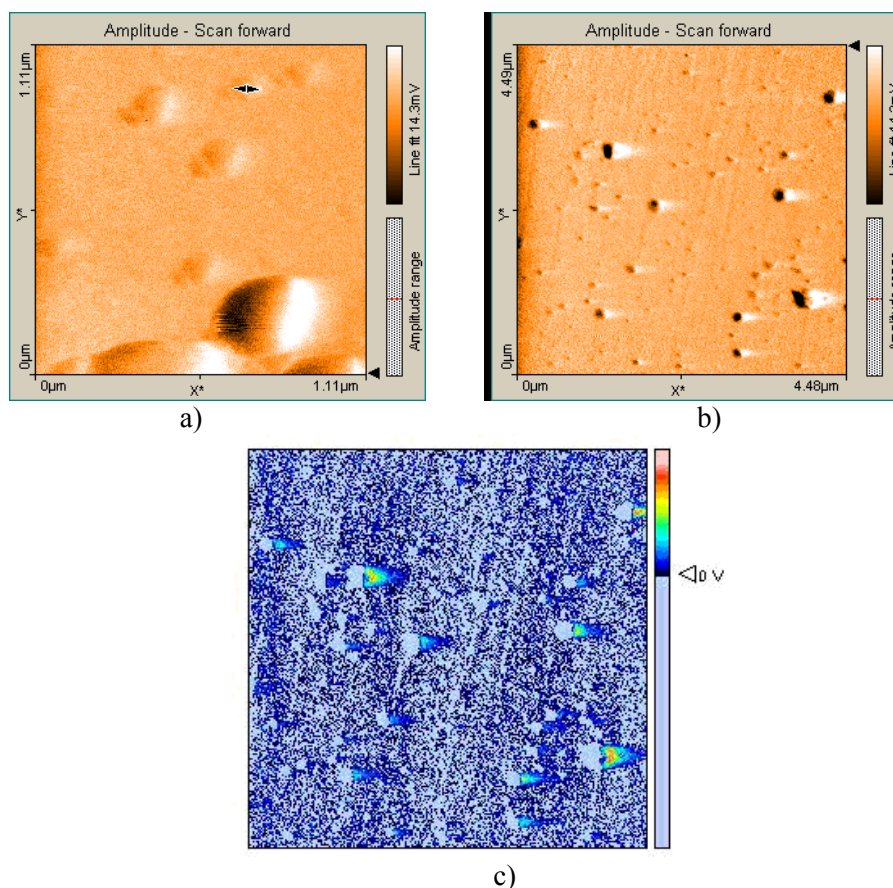


Fig. 10. 2D AFM image in contact mode and particle analysis of Sample 2 Ag colloid- complexed with (TPyDMPP) porphyrin

As expected, the number of particles is decreased at 4600 and the average height of islands is higher, around 0.51 nm and average volume of islands is larger, being of 198 nm^3 .

4. Conclusions

Colloidal systems consisting in spherical and ovoid disk-shaped silver nanoparticles in solution, with sizes in the range of 30-49 and 65-120 nm were obtained and characterized by UV-vis, fluorescence and atomic force microscopy (AFM).

New Hybrid silver colloid- A_3B porphyrin complex exhibiting wide band absorption was generated by active junction between the Ag colloids and the A_3B porphyrin, namely: 5,10,15-tris-(4-pyridyl)-20-(3,4-dimethoxy-phenyl)-porphyrin (TPyDMPP) in acidic medium. The electrostatic interactions between protonated positively charged porphyrins and the negatively charged Ag colloid explains the complex generation.

The optical properties of hybrid Ag colloid-porphyrin system, absorbing in the range of 320-770 nm, recommend them in sensors design and to be tested as photosensitizers in PDT and in photovoltaic cells. Another target was to use these materials for investigation of antibacterial performance.

Acknowledgements

The authors I. C., A. P., A. L., C. E. and E. F. G. are acknowledging the Romanian Academy, this work being part of Programme 2/2013 of the Institute of Chemistry Timisoara of Romanian Academy.

References

- [1] US Patent Appl. Pub. No. 0003603 A1, Jan. 4, 2007: Antimicrobial silver compositions
- [2] US Patent Appl. Publ. No. 0272542 A1, Dec. 7, 2006: Nanosilver as a biocide in building materials]
- [3] EU Patent: WO 2004/086044: Sensor for detecting an analyte using silver nanoparticles
- [4] D. D. Evanoff Jr., G., *ChemPhysChem*, **6**, 1221 (2005).
- [5] M. R. Das, R. K. Sarma, S. Ch. Borah, R. Kumari, R. Saikia, A. B. Deshmukh, M. V. Shelke, P. Sengupta, S. Szunerits, R. Boukherroub, *Colloids and Surfaces B: Biointerfaces* **105**, 128 (2013).
- [6] J.A. Creighton, C.G. Blatchford, M. Grant Albrecht, *J. Chem. Soc. Faraday Trans.* **75**, 790 (1979).
- [7] R. Sahraei, A. Farmany, S.S. Mortazavi, *Food Chemistry* **138**, 1239 (2013).
- [8] K. M.M. A. El-Nour, A. Eftaiha, A. Al-Warthan, R. A.A. Ammar, *Arabian Journal of Chemistry* **3**, 135 (2010).
- [9] D.L. Steed, D. Donohoe, M.W. Webster, L. Lindsley, *J. Am Coll Surg.* **183**, 6 (1996).
- [10] L. M. Liz-Marzan, *Materials' today* **7**(2) 26 (2004).
- [11] T. Angelova, N. Rangelova, R. Yuryev, N. Georgieva, R. Muller, *Materials Science & Engineering C* doi: 10.1016/j.msec.2012.03.015 (2012).
- [12] A. Taheri, M. Noroozifar, M. Khorasani-Motlagh, *Journal of Electroanalytical Chemistry* **628**, 48 (2009).
- [13] S. M. Lee, B. S. Lee, T. G. Byun, K. C. Song, *Colloids and Surfaces A: Physicochem. Eng. Aspects* **355**, 167 (2010).
- [14] M. Maillard, P. Huang, L. Brus, *Nano Lett.* **3**(11), 1611 (2003).
- [15] A. Bankar, B. Joshi, A. R. Kumar, S. Zinjarde, *Colloids and Surfaces A: Physicochem. Eng. Aspects* **368**, 58 (2010).
- [16] C. H. Ramamurthy, M. Padma, I. D. Samadanam, R. Mareswaran, A. Suyavaran, M. S. Kumar, K. Premkumar, C. Thirunavukkarasu, *Colloids Surf. B: Biointerfaces* **102**, 808 (2013).
- [17] Z. Khan, T. Singh, J. I. Hussain, A. Y. Obaid, S. A. Al-Thabarti, E. H. El-Mossalamy, *Colloids Surf. B Biointerfaces*, **102**, 578 (2013)
- [18] G. Carotenuto, G.P. Pepe, L. Nicolais, *Eur. Phys. J. B* **16**, 11 (2000).
- [19] S. Ozelik, I. Ozelik, D. L. Akins, *Appl. Phys. Lett.* **73**, 1949 (1998).
- [20] T. Vo-Dinh, *Trends in analytical chemistry* **17**, 557 (1998).
- [21] A. Šileikaite, I. Prosycevas, J. Puiso, A. Juraitis, A. Guobiene, *Materials Science (MEDŽIAGOTYRA)* **12**(4), 287 (2006).
- [22] Gh. Mihailescu, L. Olenic, S. Garabagiu, G. Blanita, E. Fagadar-Cosma, A. S. Biris, *Journal of Nanoscience and Nanotechnology* **10**, 2527 (2010).
- [23] E. Fagadar-Cosma, C. Enache, D. Vlascici, G. Fagadar-Cosma, M. Vasile, G. Bazylak, *Mater. Res. Bull.* **44**(12), 2186 (2009).
- [24] E. Fagadar-Cosma, C. Enache, I. Armeanu, D. Dascalu, G. Fagadar-Cosma, M. Vasile, I. Grozescu, *Mater. Res. Bull.* **44**(2), 426 (2009).
- [25] S. Grama, N. Hurduc, E. Fagadar-Cosma, M. Vasile, E. Tarabukina, G. Fagadar-Cosma, *Dig. J. Nanomater.Bios.* **5**, 959 (2010).
- [26] A. Ravindran, P. Chandran, S. S. Khan, *Colloids and Surfaces B: Biointerfaces* **105**, 342 (2013).
- [27] E. Fagadar-Cosma, G. Fagadar-Cosma, M. Vasile, C. Enache, *Current Organic Chemistry* **16**(24), 931 (2012).

- [28] C. H. Munro, W. E. Smith, M. Garner, J. Clarkson, P. C. White, *Langmuir* **11**(10), 3712 (1995).
- [29] Y. Xia, N. J. Halas, *MRS Bulletin* **30**, 338 (2005).
- [30] A. Slistan-Grijalva, R. Herrera-Urbina, J.F. Rivas-Silva, M. Avalos-Borja, F.F. Castillon-Barraza, A. Posada-Amarillas, *Physica E* **27**, 104 (2005).
- [31] C.F. Bohren, D.R. Huffman, *Absorption and Scattering of Light by Small Particles*, Wiley, New York, 1998
- [32] D. V. Quang, P. B. Sarawade, A. Hilonga, S. D. Park, J.-K. Kim, H. T.Kim, *Applied Surface Science* **257**, 4250 (2011).
- [33] Z. Valicsek, O. Horváth, *Microchemical Journal* **107**, 47 (2013).
- [34] G. Harrach, Z. Valicsek, O. Horváth, *Inorg. Chem. Commun.* **14**, 1756 (2011).
- [35] A. Babapour, O. Akhavan, A.Z. Moshfegh, A.A. Hosseini, *Thin Solid Films* **515**, 771 (2006).